Published in final edited form as:
*Arch Biochem Biophys*. 2008 November 15; 479(2): 105–113. doi:10.1016/j.abb.2008.08.019.

# The Structures of T87I Phosphono-CheY and T87I/Y106W Phosphono-CheY Help to Explain Their Binding Affinities to the FliM and CheZ Peptides†

**Kenneth McAdams**‡, **Eric S. Casper**‡, **R. Matthew Haas**‡, **Bernard D. Santarsiero**§, **Aimee L. Eggler**§, **Andrew Mesecar**§, and **Christopher J. Halkides**‡,*

‡ Department of Chemistry and Biochemistry, University of North Carolina Wilmington, 601 S. College Road, Wilmington, NC 28403

§ Center for Pharmaceutical Biotechnology and Department of Medicinal Chemistry and Pharmacognosy, University of Illinois College of Pharmacy, 833 S. Wood Street, Chicago, Illinois 60612-7231

## Abstract

CheY is a response regulator in bacterial chemotaxis. *E. coli* CheY mutants T87I and T87I/Y106W CheY are phosphorylatable on Asp57 but unable to generate clockwise rotation of the flagella. To understand this phenotype in terms of structure, stable analogs of the two CheY-P mutants were synthesized: T87I phosphono-CheY and T87I phosphono-CheY. Dissociation constants for peptides derived from flagellar motor protein FliM and phosphatase CheZ were determined for phosphono-CheY and the two mutants. The peptides bind phosphono-CheY almost as strongly as CheY-P; however, they do not bind T87I phosphono-CheY or T87I/Y106W phosphono-CheY, implying that the mutant proteins cannot bind FliM or CheZ tightly *in vivo.* The structures of T87I phosphono-CheY and T87I/Y106W phosphono-CheY were solved to resolutions of 1.8 Å and 2.4 Å, respectively. The increased bulk of I87 forces the side chain of Y106 or W106, into a more solvent-accessible conformation, which occludes the peptide-binding site.

### Keywords

chemical modification; structure/function studies; crystallography; fluorescence; calorimetry; chemotaxis; two component systems; protein phosphorylation

## Introduction

Prokaryotes sense and respond to a variety of environmental signals through the use of two-component systems. In these systems, an autohistidine kinase reversibly transfers a phosphoryl group to a conserved aspartate residue at the active site of the response regulator, controlling its signaling state. CheY is a single domain response regulator that functions in the chemotaxis

†Coordinates and structure factors have been deposited with the Protein Data Bank as entries 2ID7, 2ID9, and 2IDM.

*Corresponding Author: Phone (910) 962-7427, Fax (910) 962-3013, halkidesc@uncw.edu.

Manuscript prepared with Microsoft Office (Word) 2004 11.3.5.

response [1]. The histidine kinase CheA transfers a phosphoryl group from its catalytic His residue to Asp57 of CheY, creating CheY~P. CheY~P binds to the switch protein FliM at the base of the flagellar motor and changes its direction of rotation from counterclockwise, generating smooth-swimming behavior, to clockwise, generating tumbly behavior [2]. The cellular level of CheY~P is reduced by dephosphorylation, through its own autophosphatase activity as well as by the phosphatase CheZ, limiting the *in vivo* half-life of CheY~P to less than a second [3]. Changes in the concentration of CheY~P determine how frequently the periods of smooth-swimming are punctuated by tumbles; these changes can create a biased-random walk toward a better chemical environment. Mutations in CheY that bring about a greater tendency toward smooth-swimming or toward tumbly behavior impair chemotaxis [4]. CheY and CheY~P bind a divalent metal ion that necessary for both phosphorylation and dephosphorylation reactions [5]. In the structure of Mn•$BeF_3$-CheY the residues that bind to the metal ion are Asp13, Asp57, the backbone carbonyl oxygen of Asn59, and one fluorine atom [6].

*E. coli* CheY mutants T87I and T87I/Y106W CheY are phosphorylatable but cannot generate clockwise rotation of the flagella [4]. In addition, both I87 mutants have ~5-fold lower autodephosphorylation rates and are completely resistant to CheZ activity [7]. Thus, the presence of an isoleucyl side-chain at position 87 renders CheY unable to perform its chemotactic functions.

Residue 106 is an aromatic residue (tyrosine or phenylalanine) in 80% of known response regulators [8]. Matsumura and collaborators confirmed that an aromatic amino acid at position 106 is required for proper CheY~P signaling [9]. Mutagenesis and structure-function studies indicate that both the identity and the rotameric position of residue 106 are important for CheY~P signaling [4;9;10]. Substitution of Tyr106 in *E. coli* CheY with tryptophan (Y106W CheY) produces a phosphorylation-dependent, hyperactive mutant that generates mainly clockwise rotational bias [9]. Replacement of Tyr106 with a nonaromatic, nonpolar residue results in completely smooth-swimming cells that are non-chemotactic [9].

In crystals of wild-type apo-CheY, Tyr106 is found at the FliM binding surface of CheY [11; 12] and two rotameric conformations are evident from the electron density: an inside, solvent-inaccessible position and an outside, solvent-exposed position. Seminal work on the structure of $BeF_3$-CheY complexed with a peptide derived from the flagellar motor protein FliM suggested a two-state model of activation, called Y-T coupling [13]. In the uncomplexed state T87 and the β4-α4 loop are relatively distant from the active site. In the $BeF_3$-complexed form the hydroxyl group of T87 forms a hydrogen bond to one of the fluorine atoms, and Y106 moves to the solvent-inaccessible conformation. The Y-T coupling model has been expanded to include a form of CheY not posited in the original formulation, in which Y106 is solvent-inaccessible but T87 and the loop are not found in the same conformation as observed for $BeF_3$-CheY, the T-loop-Y model [14]. Structures of the complex between a peptide derived from CheZ and CheY, with and without $BeF_3$, demonstrate that T87 must move only a little to accommodate Y106 in the solvent-inaccessible rotamer [15].

Crystals of Y106W CheY show that tryptophan is found exclusively as the solvent-inaccessible rotamer [4]. In the structure of T87I CheY, Tyr106 is found only as the solvent-accessible rotamer [10]. The addition of the ethyl moiety at residue 87 sterically blocks residue 106 from occupying the solvent-inaccessible cavity. Combining these two mutations in T87I/Y106W CheY gives the same phenotype as T87I CheY [4], indicating that the T87I mutation is intragenically epistatic to the Y106W mutation. This result suggests that the buried rotamer of residue 106 is required for CheY~P to induce clockwise rotation of the flagellar motor. Mutational studies of residue 106 indicate that this residue is not required for binding between

CheY and FliM. Rather, residue 106 is critical in propagating the signal from the active site of CheY~P to FliM to elicit tumbly behavior [9].

We have sought to determine the underlying mechanism for the phenotypes of T87I CheY and T87I/Y106W CheY. Does the T87I mutation bring about a defect in *binding* between CheY~P and FliM or CheZ, or does it cause a defect in *function* without materially affecting binding? If FliM and CheZ bind to T87I CheY~P (the second possibility), phosphorylation would presumably have altered the position of I87 thus allowing residue 106 to rotate inwards. Previous structure-function studies have examined mutant CheY proteins in their *non-phosphorylated* state; however, this study is the first structure-function examination of CheY in its *phosphorylated* state. The Y-T coupling model suggests the importance of the hydrogen bond formed between the hydroxyl group of T87 and the phosphoryl group. We wished to test the hypothesis that if the side-chain at position 87 lacks the hydroxyl group, it will be not displaced as much as T87 is upon phosphorylation and will not allow rotation of the aromatic ring of residue 106.

Structural studies are difficult for CheY~P [16], which has a half-life of 15–20 s even in the absence of CheZ [17], virtually necessitating the use of some kind of analog of the active state. Several methods of mimicking the effects of phosphorylation exist, including complexing CheY with $BeF_3$ and a divalent metal ion [18] or using D13K/Y106W CheY [14]. However, no chemical analog of CheY~P has been studied with *in vivo* or *in situ* assays [19]; therefore, their biological activities are not known. Phosphono-CheY is inert to a wide variety of solution and crystallization conditions such as the presence of chelating agents, and it is nontoxic. Phosphono-CheY can be studied both in the presence and absence of a divalent metal ion [20].

In this study stable analogues of T87I CheY-P and T87I/Y106W CheY-P were prepared similarly to phosphono-CheY [21]. Fluorescence quenching of Trp58 and isothermal titration calorimetry were used to determine the affinities of these two mutants for the FliM and CheZ peptides. The FliM peptide consists of the 16 N-terminal residues of the flagellar switch protein that compose the CheY-binding region [22], and the CheZ peptide contains the 19 C-terminal residues of the phosphatase CheZ, which binds specifically to CheY~P, though at a lower affinity than that of intact CheZ [23]. Both peptides bind about 15- to 20-fold more strongly to CheY~P than to CheY [24]. The peptide studies allow us to assess whether or not the I87 mutation inhibits binding to FliM or CheZ. In addition, the structures of these proteins were determined using single-crystal x-ray diffraction. We describe the changes brought about by phosphonomethylation (to make an analog of CheY-P) of T87I CheY and T87I/Y106W CheY and examine whether phosphonomethylation or the T87I mutation controls the rotameric position of residue 106 and the conformation of the loop connecting β4 to α4, the 90s loop.

## Materials and Methods

### Protein Production, Purification, and Modification

*Escherichia coli* D57C/T87I CheY and D57C/T87I/Y106W CheY cloned into separate pet24a (+) plasmid vectors (Novagen) were gifts from Phil Matsumura. Each plasmid was transformed by standard electroporation methods into *E. coli* strain B834 (DE3) (Novagen; San Diego, CA). Purification of CheY mutant proteins were performed as previously described [20] with minor modifications. Cells were lysed with a Fisher 550 sonic dismembrator, and 0.2 mg/mL lysozyme was occasionally added to assist in breaking the cell walls. In some cases a 2.5 by 54 cm column of Sephadex G-50-150 (Sigma-Aldrich; St. Louis, MO) was used to remove higher molecular weight impurities that remained after the DE52 anion-exchange column and the Affigel Blue (Bio-Rad; Hercules, CA) column.

Phosphonomethylation of purified D57C CheY variants was performed as previously described [20] with minor modifications. Prior to the reaction between CheY and phosphonomethyltriflate, the protein was reduced with 5 mM bis(2-mercaptoethyl)sulfone for up to one hour. CheY protein was exchanged into buffer consisting of 300 mM AMPSO, pH 9.10 with 1 mM EDTA, and strontium chloride or other divalent metal chloride was added to a final concentration of 150–250 mM. An aliquot of ethanol or isopropanol (equal in volume to the volume of triethylamine) was added to phosphonomethyltriflate, then an aliquot of triethylamine consisting of 2.8 moles per mole of phosphonomethyltriflate was mixed in, and this solution was quickly added to the solution of protein with divalent metal ion. The final concentration of phosphonomethyltriflate was 95 to 140 mM. The modification reaction proceeded for 30 minutes, then 10 mM DTT was added. The protein was exchanged into 50 mM BES, pH 7.1 with 2 mM EDTA. At this point the reaction mixture was sampled for RP HPLC and DTNB assays and was roughly 65% complete, though the extent of reaction was variable. Each mixture of phosphono-CheY and D57C CheY (approximately 250 μM total concentration) was reacted with 2-3 mM PEO-maleimide biotin (Pierce Biotechnology; Rockford, IL) for 5–12 hrs to attach a biotin group and spacer to unmodified Cys57 residues. Subsequent work has suggested that 2-3 mM PEO-iodoacetyl biotin (Pierce) in 50 mM AMPSO pH 9.0 gives better results [21]. The mixture of biotinylated D57C CheY and phosphono-CheY was passed over immobilized monomeric avidin (Pierce) to remove biotinylated D57C CheY. Purified phosphono-CheY was concentrated in centricon-3 concentrators (Millipore; Billerica, MA). T87I phosphono-CheY was also purified from the crude reaction mixture by cation-exchange HPLC. A 2.5 × 200 mm ID PolyPropyl Aspartamide weak anion-exchange column (PolyLC Inc.; Columbia, MD) was equilibrated in the acetate form with 10 CV of 300 mM Na-acetate in 10 mM Tris-acetate, pH 7.0 (mobile phase B) followed by a rinse with 10 CV of 10 mM Tris-acetate, pH 7.0 (mobile phase A). The protein was loaded at 1.0 mL/min in mobile phase A and eluted on a 30 minute gradient of 0–100 % mobile phase B and the effluent monitored at 280 nm. T87I phosphono-CheY eluted approximately 3 minutes after unmodified CheY.

## X-ray Crystallography

Crystallization was performed by hanging-drop vapor diffusion. All buffers were filtered through a 0.45 μm membrane except for PEG solutions, which were filtered through a glass fiber filter with binder resin, type AP 15 (Millipore). 1.5 μL of 13–14 mg/mL protein in 5 mM Tris, 0.5 mM EDTA were mixed with 1.5 μL of well solution to form the hanging drop on a silanized cover slip. Small needle-like crystals of T87I phosphono-CheY were grown in 28% PEG 3400, 0.2 M ammonium chloride and 0.1 M sodium acetate, pH 4.60. T87I/Y106W phosphono-CheY crystal 3 was grown in 20% PEG 8000, 0.2 M ammonium acetate and 0.1 M MES-NaOH, pH 5.84. Crystal 4 of T87I/Y106W phosphono-CheY was grown in 20% PEG 8000, 0.2 M ammonium acetate and 0.1 M MES-NaOH, pH 5.88. These two crystals of the double mutant were collected and integrated separately. Since each data set showed low completeness, the intensities were combined, scaled, and averaged into one composite data set. The data collection statistics are shown in Table 1.

Typically, crystals were soaked briefly in a solution containing all well components in 10% glycerol, frozen in a stream of dry nitrogen, and intensity data collected at 100 K. Data for T87I phosphono-CheY were collected on a Rigaku/MSC R-axis IIc area detector. Data for T87I/Y106W phosphono-CheY were collected on beam line 14BMC at the Advanced Photon Source, Argonne National Laboratory, using an ADSC Quantum-4 detector. Data were processed using the program HKL [25].

The structures were solved by molecular replacement with phosphono-CheY [26] as the starting model. A test set of 5% of the total reflections were withheld from refinement and used

to calculate $R_{free}$. Iterative rounds of B-factor and positional refinement were carried out with the program CNS [27]. Toward the end of the refinement cycles, waters were added and a small fraction of the side chains were modeled in two conformations. The models were validated with the programs Molprobity [28], ProCheck [29], and What-If [30]. Table 1 contains crystallographic data and refinement statistics for both structures.

## Peptide Binding Studies

The binding of the various phosphono-CheY derivatives to peptides derived from FliM and CheZ was studied by fluorescence quenching experiments as previously described [24] and by isothermal titration calorimetry (ITC). The FliM peptide consisted of the 16 N-terminal residues of the full-length protein (MGDSILSQAEIDALLN) and the CheZ peptide consisted of C-terminal residues 196-214 (AGVVASQDQVDDLLDSLGF). Peptides were purchased from Global Peptide, Inc. Additional peptide was synthesized at the University of North Carolina Microprotein Sequencing and Peptide Synthesis Facility as needed.

In the fluorescence experiments the phosphono-CheY samples were titrated with 5 mM and 10 mM stock solutions of the FliM peptide and the CheZ peptide, respectively. Sodium hydroxide to final concentrations of 15 mM and 40 mM were added to the FliM and CheZ peptides, respectively, to obtain a pH of about 7. Solutions of CheY protein were prepared with 50 mM NaCl in 5 mM Tris or 50 mM BES, pH 7. The peptide and CheY solutions were centrifuged to minimize particulates.

Fluorescence measurements were taken on a Fluoromax spectrofluorometric detector. The experiments were carried out in a 1-mL quartz cuvette containing approximately 2 μM protein in 100 mM HEPES, 10 mM $MgCl_2$, and 0.1% sodium azide. The buffer solution had been filtered through a 0.22-μm syringe filter. The excitation wavelength was 292 nm and the emission wavelength was 345 nm. Slit widths for both excitation and emission wavelengths were 2 nm. A dust-free glass coverslip was used to cover the cuvette during the titration. The temperature was held at 25 °C, and the cuvette was allowed to equilibrate for 6–8 minutes between each addition of peptide. The uncertainty in any single measurement of fluorescence intensity was about 4% due to noise.

For ITC the peptides and the CheY proteins must be in the same buffer to avoid a significant heat of dilution. However, as the peptides were not highly soluble in the buffer used for the fluorescence experiments without the addition of sodium hydroxide, a different buffer was chosen. A 200 mM MOPS buffer, pH 7.1 with 10 mM $MgCl_2$ was found to fully solubilize the peptides at 1.5 mM without the addition of sodium hydroxide, a suitable concentration for the peptides for injection in the ITC experiments. The CheY proteins were dialyzed in this buffer, with three buffer changes, and a final dialysis step of 18 h. The final dialysate solution was filtered and used to solubilize the peptides. All ITC experiments were performed on the VP-ITC system from Microcal (Northampton, MA) using fully degassed proteins. Phosphono-CheY or T87I phosphono-CheY (21 μM) was loaded into the sample cell (volume ~1.3 mL), and the peptide (1.5 mM) was loaded into the syringe. The concentration was verified for each protein dilution using the molar extinction coefficient. All experiments were performed at 25 °C after a 300 s initial delay with 1 injection at 2 μL followed by 27 injections at 10 μL, spaced by 260 s. Experiments were performed in duplicate. Results were analyzed with MicroCal Systems analysis software (Origin 5.0), using a 1-site binding model. The n value was fixed to 1 based on the known binding stoichiometry. Fixing n has been shown to yield accurate results for similarly shaped binding isotherms [31]. Confirming this approach, the values obtained from the duplicate experiments were precise, and the equilibrium constants show good agreement with those obtained by fluorescence. The errors reported are those returned by the MicroCal Origin analysis.

### Magnesium binding study

The binding of $Mg^{2+}$ to phosphono-CheY derivatives was studied by fluorescence quenching essentially as described [32].

### Fluorescence Data Handling

Corrections were made for the added fluorescence due to the impurities in the peptide. The data were also corrected for dilution of the solution as peptide was added. Fluorescence due to the peptide impurities was first subtracted from the observed fluorescence $F_{obs}$ at a given concentration $L_t$ (total concentration of peptide in the cuvette) according to:

$$F_{corrL}=F_{obs}-f_b*L_t \tag{1}$$

where $f_p$ is the fluorescent signal (per unit concentration of peptide) due to the peptide impurities only, which was obtained by titrating the peptide into buffer with no protein. $F_{corrL}$ is the fluorescent signal due to the protein only. The $F_{corrL}$ at each concentration $L_t$ of peptide was then dilution-corrected according to:

$$F_{corr}=F_{corrL}*\frac{(V_o+V_a)}{V_o} \tag{2}$$

where $V_o$ is the initial volume of the solution in the cuvette and $V_a$ is the volume of added peptide stock solution. The corrected fluorescence data were fitted to the hyperbolic ligand-binding function:

$$\Delta F=\frac{L*\Delta F_{\max}}{K_d+L} \tag{3}$$

where $\Delta F$ is the difference between the fluorescent intensity with no peptide in solution $F_0$ and the intensity at a concentration of free peptide L. $\Delta F_{max}$ is the difference in fluorescent intensity between that at $L_t = 0$ and when all the protein is bound to peptide. $K_d$ is the dissociation constant between the protein and peptide. Since the value of L is the free peptide concentration, and $L_t$ is the sum of the concentrations of free peptide and peptide bound to the protein, L was expressed in terms of the total peptide concentration $L_t$ and the total protein concentration $M_t$, which are both known quantities [33].

$$L=0.5*\{L_t-K_d-M_t+\sqrt{(L_t-K_d-M_t)^2+4L_t*K_d}\} \tag{4}$$

Additionally, since the protein concentration diminished during the titration, $M_t$ in equation (4) was expressed in terms of the initial protein concentration, $M_i$, times a dilution correction factor:

$$M_t=M_i*\frac{(C_{pep}-L_t)}{C_{pep}} \tag{5}$$

where $C_{pep}$ is the stock concentration of peptide. The dilution correction factor in equation (5) is equivalent to the reciprocal of the dilution correction factor employed in equation (2). The

data consisting of corresponding values of $L_t$ and $F_{corr}$ (with $\Delta F = F_0 - F_{corr}$) were fitted to the composite function of expression (5) into (4), then the result substituted into (3) using KaleidaGraph (Synergy Software) least squares regression software. No attempt was made to correct for the inner filter effect or nonlinear change of fluorescence of the peptide because the maximum absorbance was kept low enough so that these effects could be ignored without significant errors.

## Results

### Binding Properties of phosphono-CheY Derivatives

The affinities of phosphono-CheY and two other CheY proteins, T87I phosphono-CheY and T87I/Y106W phosphono-CheY, for the FliM-derived peptide and the CheZ-derived peptide were determined by quenching of the fluorescence of W58 (Table 2). We observe an approximately 17-fold increase in the affinity of the FliM peptide for phosphono-CheY as compared to that for CheY, slightly higher affinity than what we previously reported [26]. Compared to phosphono-CheY, CheY~P binds the same FliM peptide with slightly higher affinity (Table 2) [24]. Likewise, phosphono-CheY and CheY~P bind the CheZ peptide with higher affinity than CheY. In sharp contrast to phosphono-CheY, T87I phosphono-CheY and T87I/Y106W phosphono-CheY showed no change in fluorescence apart from noise for either the FliM or CheZ peptide, even upon addition of 500 μM peptide in the fluorescence quenching experiments (Table 2), suggesting that there is negligible binding affinity for either the FliM or CheZ peptide for T87I mutants of phosphono-CheY.

To confirm the fluorescence quenching results and verify that the T87I mutation is indeed abolishing peptide-CheY binding, isothermal titration calorimetry experiments were carried out with phosphono-CheY and T87I phosphono-CheY with the FliM and CheZ peptides (Table 2). On the basis of several crystal structures of CheY•peptide complexes, the data were fit assuming 1:1 stoichiometry of binding [31]. As shown in Figure 1, the binding enthalpy observed for the wild type protein is clearly abolished by the T87I mutation, consistent with the fluorescence quenching result. The dissociation constants for phosphono-CheY with the CheZ and FliM peptides were 42 μM and 21 μM, respectively, similar to the values observed by quenching of fluorescence. The ΔH values obtained for phosphono-CheY with the CheZ and FliM peptides were −4.8 ± 0.3 kcal/mol and −2.4 ± 0.2 kcal/mol.

Fluorescence quenching was also used to determine the strength of binding of $Mg^{2+}$ to phosphono-CheY, T87I phosphono-CheY, and T87I/Y106W phosphono-CheY. The dissociation constants are 7 mM, 4 mM, and 7 mM, respectively. In contrast, the $K_d$ between unmodified D57C/T87I CheY and $Mg^{2+}$ is 27 mM.

### General Description of Crystallographic Results

The proteins crystallized in the $P2_12_12_1$ space group with 1 molecule per asymmetric unit. The final model of T87I phosphono-CheY refined to 1.75 Å contains 128 residues with 983 atoms and 116 water molecules. The final model of T87I/Y106W phosphono-CheY refined to 2.4 Å contains 128 residues with 985 atoms and 34 water molecules. The structures refined with good chemical geometries, and the Ramachandran plots showed that all residues fell within the allowed region, except for Asn62, the central residue of the conserved γ-turn as previously described [8]. Structural statistics and refinement data are given in Table 1.

### Overall Comparison of T87I CheY with T87I phosphono-CheY

The overall changes upon phosphonomethylation are rather modest. Superposition of Cα coordinates of T87I phosphono-CheY with molecules A and B of T87I CheY yields root mean square deviations of 0.55 Å and 0.49 Å, respectively, slightly higher than the 0.38 Å RMSD

observed *between* T87I CheY molecules A and B [10]. The side-chains of 4 glutamate and 3 lysine residues are found in multiple conformations, but these are all solvent exposed side-chains.

δ-distance mapping (Figure 1 in the supporting information) indicates that residues 88-94 shift towards the active site upon phosphonomethylation, consistent with the changes observed in the structure of $BeF_3$•CheY relative to apoCheY. When the Cα atoms of residues least affected by phosphonomethylation of T87I CheY (residues 10-86) are superposed, the most significant differences are seen in the 90's loop between β–strand 4 and helix 4. Lys91 shows the greatest displacement (2.0 Å) between corresponding Cα atoms. In T87I phosphono-CheY there is a second hydrogen bond between Glu89 Oε and Lys91 Nε in addition to the hydrogen bonding already described for T87I CheY between the backbone carbonyl of Glu89 and backbone amide of Lys91 [10]. It is not known whether or not this hydrogen bond is present in T87I CheY. The positions of the atoms in the 90's loop in T87I CheY and T87I phosphono-CheY structures differ by greater than 1.5 Å, demonstrating that this loop can attain various conformations in different structures (Figure 2 in the supporting information). Intermolecular contacts involving residues 91-98 are reported for T87I CheY [10], and T87I phosphono-CheY has a crystal contact at Ala90 which may contribute to the differences observed here; however, temperature factors for residues within the 90's loop of both structures are higher than nearby residues indicating this region has greater flexibility.

## Structure at the Active Site of T87I phosphono-CheY

Two distinct regions of electron density define the position of the phosphonomethyl moiety in the structure of T87I phosphono-CheY and are herein referred to as rotamers Pcy57 A and Pcy57 B (Figure 2). Pcy57 A resembles the phosphonomethyl group in T87I/Y106W phosphono-CheY (see below) and is intermediate between the positions of Pcy57 B and the phosphonomethyl group in phosphono-CheY [26]. A phosphoryl oxygen in Pcy57 A is 2.8 Å from Lys109 Nε but is ~ 4 Å from the backbone amides of Trp58, Asn59, and Ala88 (Table 2 in the supporting information). Pcy57 B is close to Asn59 (2.7 Å and 4.0 Å, respectively, from the two closest oxygen atoms of the phosphoryl group to the backbone amide group of Asn59); however, it is ~ 3.5 Å from Lys109 Nε and the backbone amides of Trp58 and Ala88. Therefore, both Pcy57 A and Pcy57 B occupy distinct positions from the $BeF_3$ group in $BeF_3$-CheY, in which one observes hydrogen bonds to the backbone amide groups of W58, N59, and A88, as well as the amino group of K109 [6].

In T87I phosphono-CheY the C-alpha carbon of Ile87 is positioned ~0.5 Å closer to the C-alpha carbon of residue 57 than it is in T87I CheY despite the lack of the hydroxyl group of Thr87; however, the two residues are not in contact. The hydroxyl group of T87 makes a critical hydrogen bond to a fluorine atom at the active site in $BeF_3$•CheY [6]. A solvent molecule, water82, interacts with Asn59 CO, Asp13 Oδ, a phosphoryl oxygen, and up to three other side-chains or water molecules. It is similar to water molecules observed in the apo-CheY structure [34] and the CheY•CheZ peptide structure [35], neither of which has a divalent metal ion.

## Overall Comparison of T87I/Y106W CheY with T87I/Y106W phosphono-CheY

X-ray diffraction data from two crystals of T87I/Y106W phosphono-CheY was refined to 2.4 Å (Table 1). The overall RMSD of Cα coordinates of this structure compared with T87I/Y106W CheY is 0.51 Å, which is slightly greater than the 0.42 Å RMSD observed between molecules A and B of T87I/Y106W CheY [4]. Side-chain conformations in the core of the molecule are very similar in T87I/Y106W phosphono-CheY and T87I/Y106W CheY, but variations are seen in the charged, solvent-exposed residues. Phosphonomethylation does not bring about large-scale conformational changes in T87I/Y106W CheY, but it does cause changes in the 60's loop (residues 59-64) and the 90's loop (residues 88-91). A δ-distance plot comparing T87I/Y106W

phosphono-CheY with T87I/Y106W CheY indicates the loop around residue 60 moves ~1 Å away from helix 2 (Figure 3 in the supporting information). Differences are also observed in the 90's loop, albeit smaller than is observed for T87I phosphono-CheY (Figure 2 in the supporting information). The main differences are observed in the β4-α4 portion of the loop (residues 87-89) where ~1 Å separates respective Cα atoms; however, the pseudodihedral angle defined by the Cα atoms of residues 87 through 90 does not change appreciably upon phosphonomethylation (Table 1 in the supporting information). Overall, phosphonomethylation produces similar conformational changes for the T87I/Y106W mutant as it does for the T87I mutant.

### Structure at the Active Site of T87I/Y106W phosphono-CheY

The phosphoryl group in T87I/Y106W phosphono-CheY is found in a distinct position, relative to the same group in phosphono-CheY and T87I phosphono-CheY (Figure 2) but occupies a position similar to that of $BeF_3$ in the structure of $BeF_3$-CheY [6]. The hydrogen bonds between oxygen atoms of the phosphoryl group and Trp58 NH, Asn59 NH, Ala88 NH, and Lys109 Nε implied by the structure of $BeF_3$•CheY [6] appear to be longer in T87I/Y106W phosphono-CheY (Table 2 in the supporting information). Figure 3 shows that the positions of D12, D13, residue 57 and K109 are similar when T87I phosphono-CheY and T87I/Y106W phosphono-CheY are superimposed on FixJ-P [36], suggesting that T87I/Y106W phosphono-CheY preserves most of the active-site structure of a phosphorylated response regulator, except at residue 87. This result is further evidence that phosphonomethylation is a good mimic of phosphorylation.

### Position of Residue 106 in the two mutants

A necessary part of the activation of CheY-like response regulators is the rotation of residue 106 from the g- (solvent-accessible conformer) to a g+ (solvent-inaccessible) conformer. This is evident by the change in the dihedral angle $\chi_1$ from 88.4° in apo-CheY to −174° in phosphono-CheY. In T87I CheY, the side-chain of Y106 is solvent-exposed (Figure 4a), whereas in Y106W CheY the side-chain of W106 is solvent-inaccessible [4]. In T87I/Y106W phosphono-CheY Trp106 remains in a solvent exposed conformation (Figure 4b), forced out by the increased bulk of Isoleucine 87 as described for T87I/Y106W CheY [4]. In the phosphono-CheY structures presented here, the T87I mutation prevents the aromatic ring Y106 or W106 from rotating into the hydrophobic cavity between helix 4 and β-sheet 5 (Figure 4b).

## Discussion

### Summary

Previous studies of T87I and T87I/Y106W CheY indicated that their phosphorylated forms are relatively resistant to phosphatase CheZ and fail to produce clockwise bias in the flagellar motor [4]. In order to discriminate between a failure of the phosphorylated forms of CheY to bind partner proteins and a failure to interact productively when bound, we assessed the binding between three variants of phosphono-CheY and peptides derived from CheZ or FliM. The peptide binding results confirm that phosphono-CheY is a good mimic of CheY~P (Table 2). In contrast, the FliM peptide shows no affinity for either T87I phosphono-CheY or T87I/Y106W phosphono-CheY, the former as gauged by two independent techniques. Similar data are obtained for the binding of the CheZ peptide to the various forms of CheY: the peptides bind only to phosphono-CheY, not to the two mutant forms of phosphono-CheY. These results indicate that the T87I mutation prevents binding to either peptide and that the Y106W mutation is unable to reinstitute binding ability.

To further explain the results from our peptide binding studies and the phenotypes of these mutants, we have generated crystal structures of T87I phosphono-CheY and T87I/Y106W

phosphono-CheY. The structures of T87I phosphono-CheY and T87I/Y106W phosphono-CheY demonstrate that the β4-α4 loops of CheY mutants T87I and T87I/Y106W do not assume the active conformation upon phosphorylation as described by the structure of $BeF_3$•CheY [13]. Additionally, the position of residue 106 in these CheY mutants is exclusively solvent-accessible. These results imply that the hydroxyl group of residue 87 is necessary for a change in conformation of the β4-α4 loop. Therefore, these results are consistent with the Y-T coupling model of activation and with the T-loop-Y model [14]. In addition to the lack of activation observed with T87I phosphono-CheY and T87I/Y106W phosphono-CheY, it appears that the solvent-accessible conformation of residue 106 sterically interferes with FliM and CheZ binding. These binding data and structures offer a more definitive explanation for the phenotypes of *E. coli* mutants T87I CheY and T87I/Y106W CheY than one based solely on the structures in the unphosphorylated form.

## Binding studies

The dissociation constants of the CheZ peptide to phosphono-CheY are within a factor of two greater than the dissociation constant to CheY-P, and the dissociation constants of the FliM peptide to phosphono-CheY and CheY-P are almost identical, confirming that phosphono-CheY is very similar to CheY-P in peptide binding affinity. The use of two independent techniques confirms that neither peptide has measurable affinity for T87I phosphono-CheY mutants. The binding of a peptide to T87I-mutants of CheY could fail to produce a quench in fluorescence or that binding could occur with an enthalpy of zero. Either situation would produce undetected binding, but the use of two unrelated techniques strengthens the interpretation that no binding is taking place.

The dissociation constants between $Mg^{2+}$ and the three phosphono-CheY variants studied here are essentially equal, and they indicate that the phosphono-CheY•$Mg^{2+}$ complex is the predominant form in solution in the peptide binding studies. The presence of magnesium ion may explain the modest twofold increase in affinity between phosphono-CheY and FliM reported here versus our previous determination [26]. In addition, a phosphonomethyl group provides about fivefold greater affinity for $Mg^{2+}$ than a thiol group at residue 57. Wild-type CheY binds $Mg^{2+}$ with a dissociation constant of 1 mM [32]. The half-maximal concentration for $Mg^{2+}$ quenching the fluorescence of Trp58 under phosphorylating conditions is 0.2 mM [37]. The apparent increase in affinity between wild-type CheY and $Mg^{2+}$ upon phosphorylation parallels what we observed upon phosphonomethylating Cys57.

The similarity among the dissociation constant for the three phosphono-CheY variants and $Mg^{2+}$ implies that the isoleucine side-chain does not affect the ability of the active site to bind a divalent metal ion. In addition, it suggests the active site of T87I phosphono-CheY mutants is not significantly different from other activated response regulators. Consistent with this observation, overlay of the two T87I phosphono-CheY mutants with FixJ-P shows good correlation of the active side residues involved in binding a metal ion (Figure 3). Only residue 87 and Lys109 show differences in position.

## Phenotypes of mutants

Based on our peptide binding studies, the simplest explanation for the phenotypes of these two mutants is that T87I CheY~P and T87I/Y106W CheY~P fail to bring about clockwise rotation of flagella because they cannot bind FliM *in vivo*. With respect to chemotactic behavior, Matsumura and collaborators argued that binding between CheY and FliM is necessary but not sufficient for signaling [9]. Other studies of residue 106 suggested that this residue does not alter the affinity of CheY~P for FliM but merely acts to propagate the signal after CheY~P·FliM association [4]. For example, one possible post-binding role of residue 106 is to interact with Cδ of Ile95 [38]. Our results do not exclude an additional role for residue 106.

T87I CheY~P and T87I/Y106W CheY~P are resistant to CheZ-promoted phosphatase activity [7], and the same is true of T87C CheY~P [39]. Our results suggest that a lack of affinity between T87I or T87I/Y106W CheY and CheZ is responsible for the lack of CheZ-promoted hydrolysis. In analogy with the results for FliM, a decrease in binding affinity between the T87I mutants of CheY and CheZ is the simplest explanation for decreased CheZ-catalyzed phosphatase activity. However, we cannot exclude the possibility that the T87I mutation also affects CheZ-promoted hydrolysis in other ways, for example to reposition the Glu89 side-chain [40].

## Structures

In the Y-T coupling model the hydroxyl group of T87 forms a hydrogen bond to the phosphoryl group of residue 57, bringing T87 closer to the active site [6]. However, the side-chain of Ile87 lacks a hydroxyl group, and this may explain why phosphonomethylation produces no change in the position of Ile87 relative to residue 57 for either mutant. Our results are consistent with a key role for this hydrogen bond in the activation process. Comparison of the structures of CheY and phosphono-CheY shows that the side-chain of Y106 moves from occupying either the solvent-accessible or the solvent-inaccessible conformation in the absence of the phosphoryl group at residue 57 to being exclusively solvent-inaccessible in its presence [26]. In contrast, the aromatic ring of residue 106 is exclusively in the solvent-accessible conformation in the X-ray crystal structures of T87I CheY and T87I/Y106W CheY [4;10], and phosphonomethylation does not alter its position at all, unlike the case for the wild-type protein (Figure 4). The bulkiness of side-chain of I87 outweighs any tendency from phosphonomethylation to bring the aromatic side-chain of residue 106 into its solvent-inaccessible conformation. I87 mutants of CheY are unlike D13K/Y106W CheY in this respect, where the aromatic ring is found in the solvent-accessible conformation for the free protein but can easily rotate to the solvent-inaccessible conformation when the protein binds the FliM peptide [14].

A structure of $BeF_3$•CheY in complex with the FliM peptide displays a hydrophobic contact between the peptide and Y106, the side-chain of which adopts the solvent-inaccessible conformation [13]. When the structure of this complex is superposed upon T87I phosphono-CheY, the FliM peptide clashes sterically with the aromatic side-chain of Y106, which must adopt the solvent-accessible conformation. In further support, the solvent-accessible conformation of W106 in D13K/Y106W CheY would also sterically clash with the FliM peptide [38]. The structures of the complex between $BeF_3$•CheY and the CheZ peptide are similar to the complex between $BeF_3$•CheY and FliM, except that the CheZ peptide has *two* binding modes to $BeF_3$•CheY, one of which is also observed in the $BeF_3$-free complex. In its solvent-inaccessible rotamer, the side-chain of Y106 interacts in a hydrophobic manner with the CheZ peptide in both modes, and both modes of binding are incompatible with Y106 in the solvent-accessible rotamer [35]. The hypothesis that the solvent-exposed conformation of residue 106 hinders the binding of CheY to the FliM and CheZ peptides is consistent with the structural data of these peptide-protein complexes.

In addition to the rotation of Y106, another aspect of CheY activation is a conformational shift of the 90's loop In T87I/Y106W phosphono-CheY versus T87I/Y106W CheY, a shift of the 90's loop towards helix 3 can be seen, similar in direction but smaller in magnitude than that observed for beryllofluoride-activated CheY [41] versus apo-CheY [11]. This backbone change may be responding to a putative new hydrogen bond between Glu89 Oε and Lys91 Nε (see Results) and may have functional significance inasmuch as Glu89 participates in the CheZ-promoted hydrolysis of CheY~P [40].

Although residue 106 remains in its solvent-accessible rotamer in the two phosphono-CheY mutants discussed here, this rotamer does not lock the 90's loop into a single conformation

(Figure 2, in supporting information). One parameter that has been used to describe the loop is the pseudodihedral angle defined by the Cα atoms of residues 87 through 90 [14]. Both T87I phosphono-CheY and T87I/Y106W phosphono-CheY have pseudodihedral angles that are similar to those observed for their nonphosphorylated forms, falling in the range of 13–22°. These values are somewhat less than that for phosphono-CheY, which has an intermediate pseudodihedral angle (44°), versus $BeF_3$-CheY (~110°). The conformation of the loop in phosphono-CheY resembles the loop-up conformation (loop away from Tyr106) observed for meta-active CheY (one of two conformations observed in the 1.1 Å structure of CheY), in which Tyr106 is found in the solvent-inaccessible rotamer [34]. We acknowledge that the errors in dihedral and pseudodihedral angles might be on the order of 20 degrees; however, small changes in protein structure are known to have large effects on function [42].

## Supplementary Material

Refer to Web version on PubMed Central for supplementary material.

## Acknowledgments

We thank Cory J. Bottone for technical assistance and helpful discussions. Use of the Advanced Photon Source was supported by U.S. Department of Energy, Basic Energy Sciences, Office of Science, under Contract No. W-31-109-Eng-38. Use of the BioCARS Sector 14 was supported by the National Institutes of Health, National Center for Research Resources, under grant number RR07707.

Support for this work was provided by the North Carolina Biotechnology Center ARIG Grant Number 9905ARG0026 and by the National Institutes of Health Grant Number 1R15GM063514-01A1. Its contents are solely the responsibility of the authors and do not necessarily represent the official views of the North Carolina Biotechnology Center or the NIH.

## Abbreviations

| | |
|---|---|
| CheA | product of the chemotaxis A gene |
| CheY | product of the chemotaxis Y gene |
| CheZ | product of the chemotaxis Z gene |
| CheY~P | phosphorylated form of CheY |
| EDTA | ethylenediaminetetraacetic acid |
| DTT | dithiothreitol |
| DTNB | 5,5′-dithiobis(2-nitrobenzoic acid) |
| FliM | flagellar switch protein M |
| AMPSO | 3-[(1,1-dimethyl-2-hydroxyethyl)amino]-2-hydroxypropanesulfonic acid |
| BES | N,N-bis(2-hydroxyethyl)-2-aminoethanesulfonic acid |
| RP HPLC | reversed phase high-performance liquid chromatography |
| PEG | polyethylene glycol |
| MES | 2-morpholinoethanesulfonic acid |
| Tris | tris(hydroxymethyl)aminomethane |
| HEPES | N-(2-hydroxyethyl)-piperazine-N′-2-ethanesulfonic acid |
| RMSD | root mean squared deviation |

## References


1. Matsumura P, Rydel JJ, Linzmeier R, Vacante D. J Bacteriol 1984;160:36–41. [PubMed: 6090423]
2. Baker MD, Wolanin PM, Stock JB. BioEssays 2006;28:9–22. [PubMed: 16369945]
3. Silversmith RE. Biochemistry 2005;44:7768–7776. [PubMed: 15909991]
4. Zhu X, Rebello J, Matsumura P, Volz K. J Biol Chem 1997a;272:5000–5006. [PubMed: 9030562]
5. Lukat GS, Stock AM, Stock JB. Biochemistry 1990;29:5436–5442. [PubMed: 2201404]
6. Lee SY, Cho HS, Pelton JG, Yan D, Berry EA, Wemmer DE. J Biol Chem 2001;276:16425–16431. [PubMed: 11279165]
7. Zhu X, Volz K, Matsumura P. J Biol Chem 1997b;272:23758–23764. [PubMed: 9295320]
8. Volz K. Biochemistry 1993;32:11741–11753. [PubMed: 8218244]
9. Zhu X, Amsler CD, Volz K, Matsumura P. J Bacteriol 1996;178:4208–4215. [PubMed: 8763950]
10. Ganguli S, Wang H, Matsumura P, Volz K. J Biol Chem 1995;270:17386–17393. [PubMed: 7615544]
11. Volz K, Matsumura P. J Biol Chem 1991;266:15511–15519. [PubMed: 1869568]
12. Roman SJ, Meyers M, Volz K, Matsumura P. J Bacteriol 1992;174:6247–6255. [PubMed: 1400175]
13. Lee SY, Cho HS, Pelton JG, Yan D, Henderson RK, King DS, Huang LS, Kustu S, Berry EA, Wemmer DE. Nat Struct Biol 2001;8:52–56. [PubMed: 11135671]
14. Dyer CM, Dahlquist FW. J Bacteriol 2006;188:7354–7363. [PubMed: 17050923]
15. Stock AM, Guhaniyogi J. J Bacteriol 2006;188:7328–7330. [PubMed: 17050920]
16. Lowry DF, Roth AF, Rupert PB, Dahlquist FW, Moy FJ, Domaille PJ, Matsumura P. J Biol Chem 1994;269:26358–26362. [PubMed: 7929354]
17. Hess JF, Oosawa K, Kaplan N, Simon MI. Cell 1988;53:79–87. [PubMed: 3280143]
18. Wemmer DE, Kern D. J Bacteriol 2005;187:8229–8230. [PubMed: 16321925]
19. Barak R, Eisenbach M. Biochemistry 1992;31:1821–1826. [PubMed: 1737035]
20. Halkides CJ, Zhu X, Phillion DP, Matsumura P, Dahlquist FW. Biochemistry 1998;37:13674–13680. [PubMed: 9753454]
21. Halkides CJ, Bottone CJ, Casper ES, Haas RM, McAdams K. Methods Enzymol 2007;422:338–351. [PubMed: 17628147]
22. Bren A, Eisenbach M. J Mol Biol 1998;278:507–514. [PubMed: 9600834]
23. Blat Y, Eisenbach M. Biochemistry 1996;35:5679–5683. [PubMed: 8639527]
24. McEvoy MM, Bren A, Eisenbach M, Dahlquist FW. J Mol Biol 1999;289:1423–1433. [PubMed: 10373376]
25. Otwinowski Z, Minor W, Carter Charles W Jr. Methods Enzymol 1997;276:307–326.
26. Halkides CJ, McEvoy MM, Casper E, Matsumura P, Volz K, Dahlquist FW. Biochemistry 2000;39:5280–5286. [PubMed: 10819997]
27. Brünger AT, Adams PD, Clore GM, DeLano WL, Gros P, Grosse-Kunstleve RW, Jiang JS, Kuszewski J, Nilges M, Pannu NS, Read RJ, Rice LM, Simonson T, Warren GL. Acta Crystallogr, Sect D: Biol Crystallogr 1998;54:905–921. [PubMed: 9757107]
28. Lovell SC, Davis IW, WBA, Bakker PIWd, Word JM, Prisant MG, Richardson JS, Richardson DC. Proteins: Struct, Funct, Genet 2003;50:437–450. [PubMed: 12557186]
29. Laskowski RA, MacArthur MW, Moss DS, Thornton JM. J Appl Crystallogr 1993;26:283–291.
30. Vriend G. J Mol Graphics 1990;8:52–56.
31. Turnbull WB, Daranas AH. J Amer Chem Soc 2003;125:14859–14866. [PubMed: 14640663]
32. Needham JV, Chen TY, Falke JJ. Biochemistry 1993;32:3363–3367. [PubMed: 8461299]
33. Eftink MR. Methods Enzymol 1997;278:221–257. [PubMed: 9170316]
34. Simonovic M, Volz K. J Biol Chem 2001;276:28637–28640. [PubMed: 11410584]
35. Guhaniyogi J, Robinson V, Stock A. J Mol Biol 2006;359:624–645. [PubMed: 16674976]
36. Birck C, Mourey L, Gouet P, Fabry B, Schumacher J, Rousseau P, Kahn D, Samama JP. Structure 1999;7:1505–1515. [PubMed: 10647181]
37. Welch M, Oosawa K, Aizawa SI, Eisenbach M. Biochemistry 1994;33:10470–10476. [PubMed: 8068685]

38. Dyer CM, Quillin ML, Campos A, Lu J, McEvoy MM, Hausrath AC, Westbrook EM, Matsumura P, Matthews BW, Dahlquist FM. J Mol Biol 2004;342:1325–1335. [PubMed: 15351654]
39. Appleby JL, Bourret RB. J Bacteriol 1998;180:3563–3569. [PubMed: 9657998]
40. Silversmith RE, Guanga GP, Betts L, Chu C, Zhao R, Bourret RB. J Bacteriol 2003;185:1495–1502. [PubMed: 12591865]
41. Cho HS, Lee S-Y, Yan D, Pan X, Parkinson JS, Kustu S, Wemmer DE, Pelton JG. J Mol Biol 2000;297:543–551. [PubMed: 10731410]
42. Mesecar AD, Stoddard BL, Koshland DE Jr. Science 1997;277:202–206. [PubMed: 9211842]

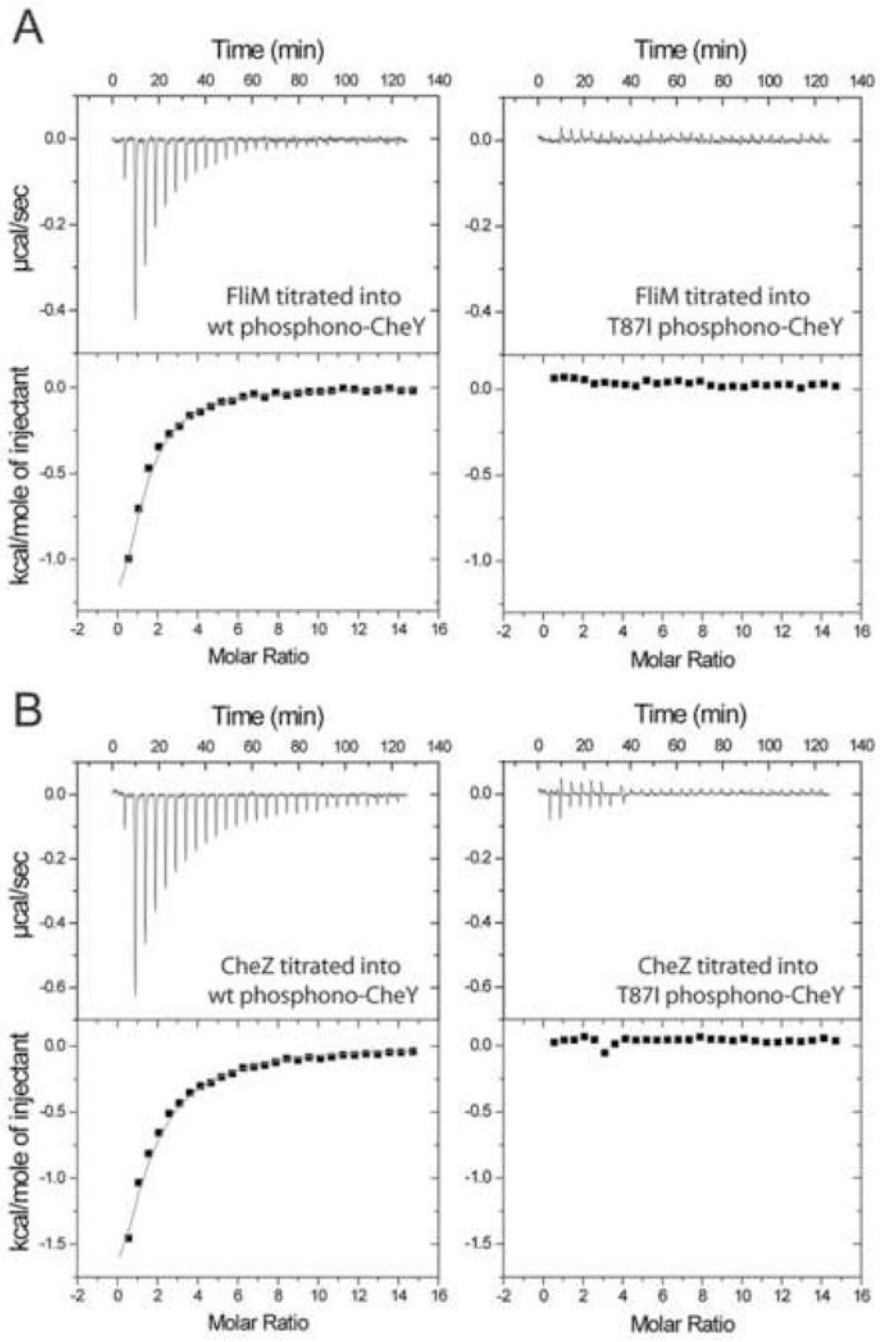


**Figure 1.**

Isothermal titration calorimetry profiles of FliM or CheZ with phosphono-CheY or T87I phosphono-CheY. Representative profiles are shown for 1.5 mM peptide titrated into 21 μM protein at 25 °C, as labeled. Upper panels represent ITC thermographs, and lower panels represent the binding isotherms. The solid squares represent data points, and the curves represent the best fit to the data, taking the stoichiometric coefficient n as unity.

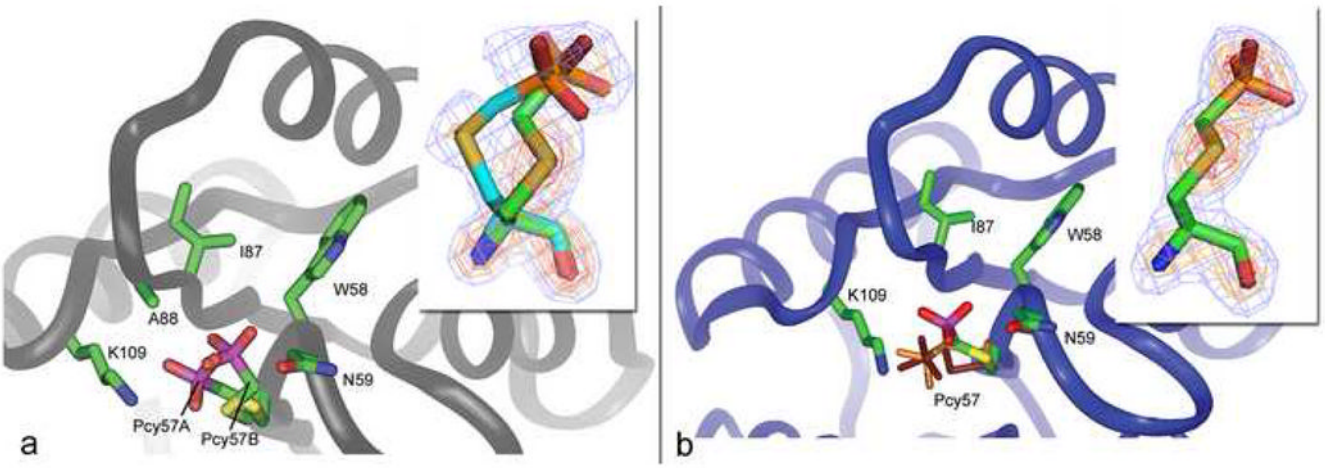


**Figure 2.**

Active sites of T87I phosphono-CheY and T87I/Y106W phosphono-CheY. Sulfur is yellow and phosphorus is purple. (A) T87I phosphono-CheY exhibits two conformations of the phosphonomethyl group, Pcy57 A and Pcy57 B; Pcy57 B is close to the backbone amide group of Asn59, and Pcy57 A is close to the amino group of Lys109. The inset shows the electron density of the side-chain of residue 57 from an omit map drawn at 4σ (blue), 6σ (amber), and 8σ (red). Sulfur is yellow, and phosphorus is orange. (B) Active site of T87I/Y106W phosphono-CheY compared to phosphono-CheY (thin brown cylinders – Pcy57A is light brown, Pcy57B is dark brown). The phosphoryl group of T87I/Y106W phosphono-CheY is closer to the amide bonds of Trp58 and Asn59 than the phosphoryl group of phosphono-CheY is. The inset shows the electron density of residue 57 from an omit map as in part A. Unlike residue 57 in T87I phosphono-CheY, this side-chain is well ordered.

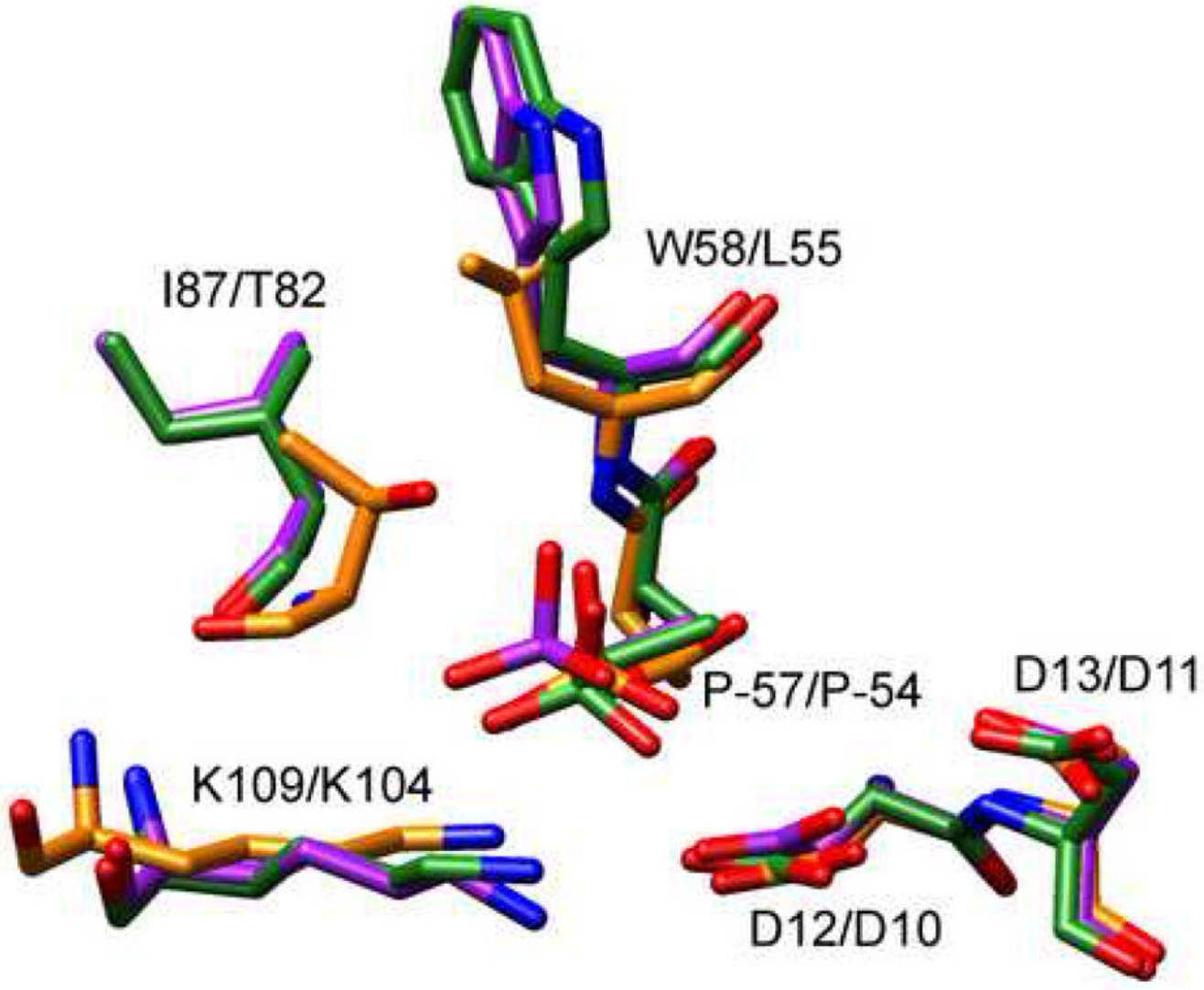


**Figure 3.**
Superposition of T87I phosphono-CheY in green (this work), T87I/Y106W phosphono-CheY in purple (this work), and FixJ-P in orange [36]. Residue numbers after the slash are from Fix-J. Most of the active site residues, including D12, D13, and residue 57 are found in similar positions. These three residues are close to the divalent metal ion in the structure of $BeF_3$-CheY, the latter two being in direct contact [6]. Ile87 in the two phosphono-CheY mutants is not as close to residue 57 as Thr87 is in the Fix-J structure.

Figure 4a

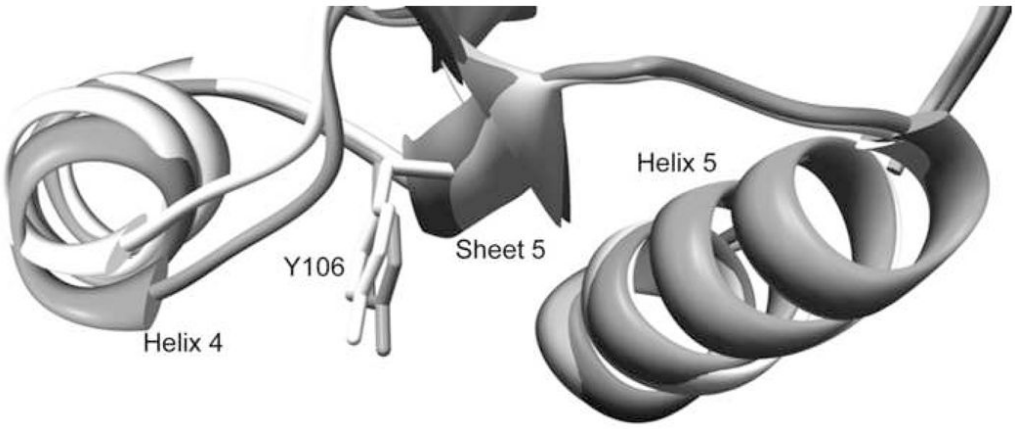


Figure 4b

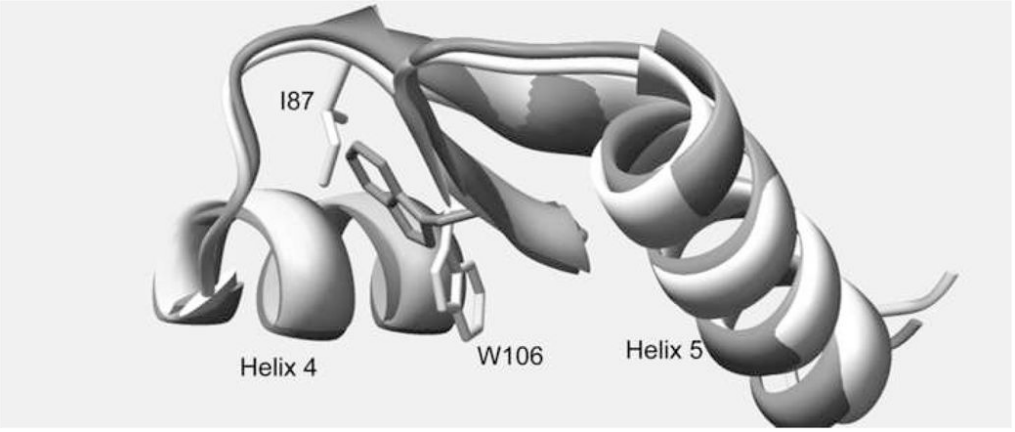


**Figure 4.**

a) Position of Y106 in T87I phosphono-CheY (white) and T87I CheY (grey). In both structures the aromatic ring is observed in its solvent-accessible rotamer. When the Y106 side chain adopts this rotameric state, it prevents binding of peptides, b) Position of W106 in T87I/Y106W phosphono-CheY (white) and Y106W CheY (grey). In Y106W CheY the aromatic side-chain is in its solvent-inaccessible rotamer, whereas in T87I/Y106 W CheY it is solvent accessible. The side-chain of I87 would clash with W106 in the solvent-inaccessible conformation in T87I/Y106W phosphono-CheY. Yet only the solvent-inaccessible rotamer is compatible with binding peptides derived from FliM or CheZ, as discussed in the text.

**Table 1**

Data Collection and Refinement Summary

| | T87I phosphono-CheY | T87I/Y106W phosphono- CheY |
|---|---|---|
| Space group | $P2_12_12_1$ | $P2_12_12_1$ |
| Unit cell dimension a, b, c (Å) | 41.35, 49.96, 53.90 | 40.14, 50.40, 53.09 |
| Refinement resolution (Å) | 20.0 – 1.85 | 20.0 – 2.40 |
| Total number collected | 99138 | 196870 |
| mosaicity | 0.46–0.65 | 1.30 |
| I/σ | 35.9 (9.6) | 25.6 (10.7) |
| Completeness (%) | 98.3 (95.8) | 97.1 (99.8) |
| $R_{sym}$ | 0.045 (0.127) | 0.078 (0.256) |
| $\chi^2$ | 1.53 (1.07) | 1.47 (1.23) |
| No. of molecules in AU | 1 | 1 |
| No. residues | 128 (6 disordered) | 128 (5 disordered) |
| No. protein atoms | 1033 | 1026 |
| No. solvent atoms | 116 | 34 |
| Total theoretical no. of reflections | 9968 | 4504 |
| No. reflections used | 9599 | 4374 |
| Reflections work - test | 9092 – 507 | 4120 – 254 |
| $R_{free}$ | 0.205 | 0.292 |
| $R_{cryst}$ | 0.167 | 0.221 |
| m | 0.894 | 0.801 |
| RMSD bond lengths (Å) | 0.016 | 0.010 |
| RMSD bond angles (degrees) | 1.88 | 1.4 |

Numbers in parentheses give the value for the highest-resolution shell

AU, asymmetric unit; m, figure of merit; RMSD, root mean square deviation; $R_{free}$ is $R_{cryst}$ over the random 5% of data set that was excluded from refinement.

$$R_{cryst}=\frac{\sum \left||F_o|-|F_c|\right|}{\sum |F_o|}$$, Fo is observed F(hkl); Fc is calculated F(hkl), sum over all hkl reflections

$$R_{sym}=\sum_{hkl}\frac{\sum_i \left||F^2_{hkl}|-|F^2_i|\right|}{\sum |F_i|}$$ sum over all observations i of reflection hkl, over all hkl reflections

$$X^2=\sum_{hkl}\sum_i \frac{(|F^2|_i-\overline{|F^2|}_{hkl})^2}{\sigma^2_{hkl}(n/n-1)}$$

$$m=\sum_{hkl}\frac{|\rho(hkl)_c|}{|\rho(hkl)_o|}$$

## Table 2

Dissociation constants in μM of peptides from CheY determined by fluorescence or isothermal titration calorimetry (ITC)

| | FliM peptide $K_d$, μM | | CheZ peptide $K_d$, μM | |
|---|---|---|---|---|
| | **Fluorescence** | **ITC** | **Fluorescence** | **ITC** |
| CheY | 680 ± 10[a] | n/d[e] | 440 ± 10[a] | n/d[e] |
| CheY~P | 27 ± 1[a] | n/d[e] | 26 ± 1[a] | n/d[e] |
| Phosphono-CheY | 38 ± 1 | 21 ± 1[c] | 58 ± 4 | 42 ± 2[c] |
| T87I Phosphono-CheY | Not detectable[b] | Not detectable[d] | Not detectable[b] | Not detectable[d] |
| T87I/Y106W Phosphono-CheY | Not detectable[b] | n/d[e] | Not detectable[b] | n/d[e] |

[a] McEvoy et al., (1999) *J. Mol. Biol. 289*, 1423–1433.

[b] No change in fluorescence intensity was observed up to 500 μM peptide concentration. The uncertainty in intensity is about 4 % due to noise.

[c] Values from one of two duplicate runs are reported. The other run gave similar values.

[d] No change in enthalpy was observed.

[e] n/d: not determined.